

Award Accounts

The Chemical Society of Japan Award for Young Chemists in Technical Development for 2002

Purified Coating Solution and Growth Scheme of the $YBa_2Cu_3O_{7-x}$ Superconductors in Metal Organic Deposition Using Trifluoroacetates

Takeshi Araki

Division of Material Science & Physics, Superconductivity Research Laboratory, 10-13, Shinonome 1-chome, Koto-ku, Tokyo 135-0062

Received September 12, 2003; E-mail: araki@istec.or.jp

Metal organic deposition using trifluoroacetate (TFA-MOD) is one of the most promising approaches to $YBa_2Cu_3O_{7-x}$ superconductors. In this process, CuO nanocrystallites in calcined film never cause random orientation, which is a major problem in the other solution processes. A "quasi-liquid network" created during the firing process suppresses the influence of the nanocrystallites on the epitaxial structure. Impurities in the coating solution cause Y, Ba, and Cu compounds; a long calcining process leads to CuO grain growth in the $YBa_2Cu_3O_{7-x}$ film. These compounds deteriorate superconducting properties in two ways. One is a direct physical obstacle and the other is an indirect chemical influence. In the latter mode, non-stoichiometric area, which is induced by the compound, breaks up the quasi-liquid and the quasi-liquid changes into the other phase. Therefore, the actual $YBa_2Cu_3O_{7-x}$ film is thinner and the superconducting properties degrade. To reduce the influence of CuO nanocrystallites, excess humidity in the firing gas is effective because increased quasi-liquid consumes the nanocrystallites. However, the improvement is imperfect. A combination of highly purified coating solution and optimal calcining process is required to obtain high performance $YBa_2Cu_3O_{7-x}$ superconductors. With such a combination, $YBa_2Cu_3O_{7-x}$ films having critical current density of 5–7 MA/cm^2 (77 K, 0 T) are routinely obtained.

Superconductors are divided into two groups: one includes metal superconductor, which have a relative low critical temperature (T_c) below 39 K; the other includes oxide superconductors. The metal superconductors require expensive liquid He to work.[1,2] Most oxide superconductors have higher T_c values than the boiling point of nitrogen, 77 K. Since liquid nitrogen is not expensive, these oxide superconductors have been studied; their applications are eagerly awaited. Among the oxide superconductors including Bi-, Y-, Hg-, and Tl-based compounds,[3] the $YBa_2Cu_3O_{7-x}$ (YBCO) superconductor has the most excellent properties in critical current density (J_c) at 77 K.[4–6] In addition the YBCO superconductor has excellent properties in high magnetic fields.[7,8] This implies strong possibilities for high magnetic field application. Therefore, YBCO coated conductors have been studied extensively.

Relatively good YBCO films have been prepared by physical routes.[4–6] The most popular method is pulsed laser deposition. In this process, a target that consists of the final materials is set on a rotating table. The laser beam is focused on the target through a lens to form a plume. The substrate must be heated on the heater to control its temperature strictly and must simultaneously be set in a proper position to deposit superconductor material well. The whole system must be kept at a reduced pressure. The expensive laser and the vacuum apparatus disturb the application of YBCO films by physical routes; in addition, the difficulties in controlling their deposition conditions lead to low reproducibility in the superconducting properties.

Thus a low-cost chemical approach of metal organic deposition (MOD) has been studied as an alternative process to overcome the above problems.[9–11] In MOD, a gel film is formed on the substrate through dip-coating or by a spin-coating process with coating solution. The gel film is calcined and fired in ambient pressure to give a superconductor. Organic materials are decomposed to become oxides during the calcining process and these oxides form epitaxial superconducting layers during the firing process. Since this MOD process requires no vacuum apparatus, production cost is dramatically reduced. However, if stable $BaCO_3$ forms in the calcined film, it is difficult to decompose.[12] Intrusion of $BaCO_3$ into YBCO structure also degrades the superconducting properties.[13] In addition, if nanocrystallites form during the calcining process, they cause random orientation in the resulting film.[14] Rapid heating is required to suppress the formation of the nanocrystallites. However, such rapid heating induces unforeseen chemical reactions and yields a harmful carbon residue in the calcined film. These phenomena result in low superconducting properties and low reproducibility of the properties.[15]

Among many kinds of MODs, one process avoids $BaCO_3$ formation, expels the carbon contents during the calcining process and causes no random orientation of the resulting fired

Published on the web June 9, 2004; DOI 10.1246/bcsj.77.1051

film. This is metal organic deposition using trifluoroacetates (TFA-MOD).[16] In this process, the long calcining process actually yields innumerable nanocrystallites in the calcined film.[17,18] Observation by transmission electron microscopy (TEM) also confirmed the results. A perfectly oriented YBCO layer is easily obtained through the firing process with extremely high reproducibility.[19] Actually, large-area YBCO films on 50 mm-diameter substrates are easily obtained[20] and about 10 m-long YBCO tapes even on buffered metal tapes[21] were reported. This TFA-MOD process is regarded as one of the most promising processes. Thus many scientists in the world have been studying this TFA-MOD process.[22–25]

TFA-MOD was initially proposed as an alternative process to the electron-beam process. Prior to the proposal, Mankiewich et al. prepared a precursor film with BaF_2 to avoid stable $BaCO_3$ formation by the electron-beam process.[26] Through the firing process under humidified gas, the precursor film changes into an excellent superconducting layer. This electron-beam process is also a kind of vacuum process. To prepare a similar precursor (calcined) film by a low-cost chemical route, Gupta et al. prepared a film by TFA-MOD process.[16] The resulting superconductors did not have such excellent properties as those of the electron-beam process,[26–28] because their starting materials inevitably increase the total amount of impurities in the coating solution. No one reported any special schemes in the TFA-MOD process, so TFA-MOD was regarded as one of the conventional MOD processes. McIntyre et al. improved the properties of TFA-MOD derived films.[17,29,30] Finally, Smith et al. reported that they obtained a 1 μm-thick YBCO film,[31] which is an extraordinary thickness in this field. Afterward, we reported that a highly purified coating solution could be obtained by Solvent-Into-Gel (SIG) method. With this solution, we prepared 50 mm-diameter YBCO films on single crystal substrates[20] and reported high-J_c results. Siegal et al. reported high-J_c film on metal tape obtained by an all-solution process,[32] where they prepared the intermediate layer by a low-cost MOD process. Furthermore, we reported a carbon-expelling scheme during the calcining process[33] and a growth mechanism of YBCO layer during the firing process.[18] These two schemes imply that TFA-MOD intrinsically yields excellent superconductors with extremely high reproducibility.

As described above, during the calcining process of TFA-MOD, harmful carbon contents are entirely expelled and an amorphous layer of Ba–O–F forms instead of $BaCO_3$. We report the detailed reason with thermodynamical studies and chemical background. Details of this scheme are described in an article published elsewhere.[33] During the firing process, nanocrystallites have no influence on the resulting structure. So the growth-limiting stage of the firing process is not the diffusion of generated HF gas between growth front and film surface, but the diffusion from the film surface. In TFA-MOD, the required firing time is simply proportional to the film thickness, while the time is proportional to the square of the thickness in conventional MOD.[34] The quasi-liquid network model solved all these unsolved problems.[18,19]

To obtain high-J_c YBCO film by TFA-MOD, one must use a purified coating solution.[20] However, such a purified coating solution for TFA-MOD is difficult to obtain. Since the most electronegative fluorine atom in trifluoroacetates forms strong hydrogen bonds with water, large amounts of impurities remain through the purifying process in water solvent. On the other hand, in alcohol solvent, esterification fatally decomposes the trifluoroacetates[35] and the non-stoichiometric coating solution never yields excellent superconductors.

In this Award Account, the detailed preparation processes used to obtain purified coating solutions are explained. The detailed growth scheme during the firing process is also explained.

Preparation Process for Purified Coating Solution

1. Difficulty in Purifying Trifluoroacetates. It is difficult to purify trifluoroacetates because the most electronegative fluorine atoms form strong hydrogen bonds with hydrogen atoms in water solvent. On the other hand, the salts esterify with alcohol solvent even at a calm condition.[35] As a result, one of the biggest vendors in the world does not provide the pure raw materials listed in Table 1. In this TFA-MOD process, we need, not the pure salts themselves, but alcohol solutions of the salts to prepare high-J_c YBCO films.[20,36] As an alternative way to obtain the purified coating solution, we have developed a three-step process to obtain the purified coating solution: firstly, we obtain the salts with impurities in non-alcohol solvent; secondly we expel the impurities to obtain the purified material with a method; and finally the purified coating solution is obtained by dissolving the material into alcohol. The process is a base-exchanging route. The weight ratio of the impurities trapped in the blue gel is about 10–12 wt % in Fig. 1. To expel the impurities effectively, we should know the main impurity and its trapping scheme.

2. Trapping Scheme of Main Impurity. In this preparation route, the only impurities are water and acetic acid. A flask including the materials is kept at 40–60 °C during the first purifying process. Partial pressures of the impurities are listed in Table 2. The partial pressure of acetic acid is calculated with the help of Antoine's equation, described by

$$\log(760/1013 \times P) = A - B/(C + t). \quad (1)$$

Here P (hPa) and t (°C) represent partial pressure of a material and its temperature, respectively. In Eq. 1, A, B, and C are constants. Their values for acetic acid are 7.42728, 1558.03, and 224.79, respectively, at 0–100 °C.[37] $P(H_2O)$ is higher than $P(CH_3COOH)$ at all temperatures during the preparation process. This purifying process requires a relatively long time of about 10 hours. This is enough time to separate water from acetic acid, with the difference listed in Table 2. From this point of view, the main impurity in the blue gel with impurities should be acetic acid. We synthesized the coating solution three times.

Table 1. List of Raw Materials from Vendors

Material	Purity/%	Number of hydrates
$(CF_3COO)_3Y$	99	x (~4)
$(CF_3COO)_2Ba$	not for sale	—
$(CF_3COO)_2Cu$	unknown	1
$(CH_3COO)_3Y$	99.999	x (~4)
$(CH_3COO)_2Ba$	99.999	0
$(CH_3COO)_2Cu$	99.99+	1

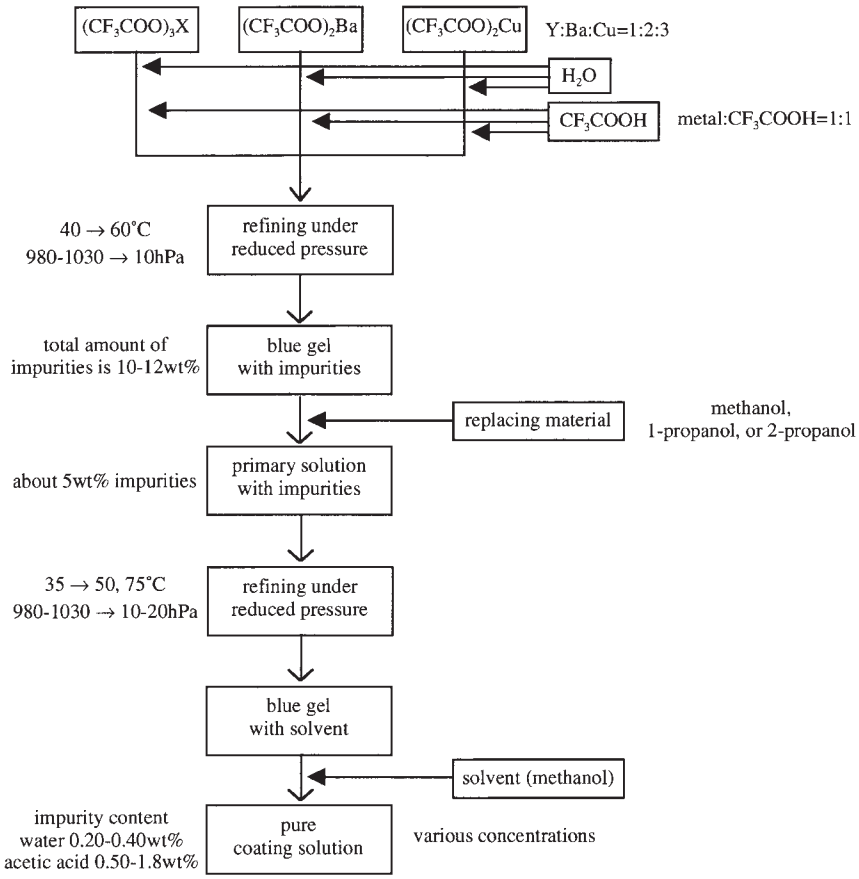

Fig. 1. Process for preparing purified coating solution in TFA-MOD. Metal trifluoroacetates are synthesized with metal acetates and trifluoroacetic acid in water. Sticky gel intrinsically confines impurities during the refining process. The impurities can be replaced with alcohol solvent. Avoiding esterification between trifluoroacetates and the alcohol solvent, the impurities can be mostly expelled with the Solvent-Into-Gel (SIG) method.

Table 2. List of Partial Pressures of Acetic Acid and Water

Temperature /°C	$P(CH_3COOH)$ /hPa	$P(H_2O)$ /hPa
30	27.4	42.4
35	35.9	56.2
40	46.6	73.7
45	59.9	95.8
50	76.2	123.4
55	96.3	157.4
60	120.6	199.2
65	149.9	250.1
70	184.9	311.6
75	226.5	385.4
80	275.6	473.5

Each time, we measured water and acetic acid contents; the results are summarized in Table 3.[38] These results were measured as amounts of impurities in coating solution. To compare the ratios of 10–12 wt % of impurities in glassy blue gel, we should know the density of trifluoroacetates for the calculation. The density is 2.37 g/cm^2 at 25 °C, calculated by comparing two kinds of coating solution with different concentrations. We use an experimental datum of 10.9 wt % as a ratio in the glassy gel to calculate the corresponding ratio in coating solution. Ignoring the slight volume decrease that occur on mixing materials, the ideal weight of trifluoroacetates in 1.50 mol/L of ionic concentration in 100 mL is 50.77 g, as listed in Table 4. Using the above impurities ratio, one can estimate the sweight of the impurities to be 5.53 g. The density of acetic acid is 1.049 g/cm^3, which is similar to that of water. The volume of the impurities is estimated to be 5.27 cm^3 in the case of pure acetic acid and to be 5.53 cm^3 in the case of pure water. The difference of the two data is only 0.26 cm^3, which is negligible compared with the total volume of 100 cm^3. Here, we use 1.000 g/cm^3 as the density of the impurities. Substituting the volume of trifluoroacetates and impurities, we identify a volume of methanol solution. Based on the data, an equivalent ratio of impurities to coating solution is estimated to be 4.85 wt %, as listed in Table 4. Compared with the datum of 4.85 wt %, the total amount of impurities listed in Table 3 is lower by approximately 20%. However, we conclude that the data are reliable enough to identify a major impurity in the blue gel with impurities.

Table 3. List of Impurities in Primary Solution

Solution	CH_3COOH /wt %	H_2O /wt %
A	0.82	3.4
B	0.93	3.1
C	0.85	3.2

Table 4. List for Calculated Equivalent Impurities Ratio in a Coating Solution

Content	Amount	Unit
ideal blue gel weight	50.77	g
ratio of impurities	10.9	wt %
weight of impurities	5.534	g
density of trifluoroacetates	2.37	$g\,cm^{-3}$
density of acetic acid	1.049	$g\,cm^{-3}$
density of water	1.000	$g\,cm^{-3}$
density of methanol	0.79142	$g\,cm^{-3}$
volume of the gel	21.42	cm^3
volume of impurities	5.27	cm^3
volume of solvent	73.04	cm^3
total weight of solution	114.11	g
impurities ratio of solution	4.85	wt %

Table 5. List of Impurities and Replacing Materials in Coating Solution

Solution	CH_3COOH /wt %	H_2O /wt %	1-Propanol /wt %	2-Propanol /wt %
D	1.70	0.26	7.0	0.0
E	1.77	0.39	0.0	9.8

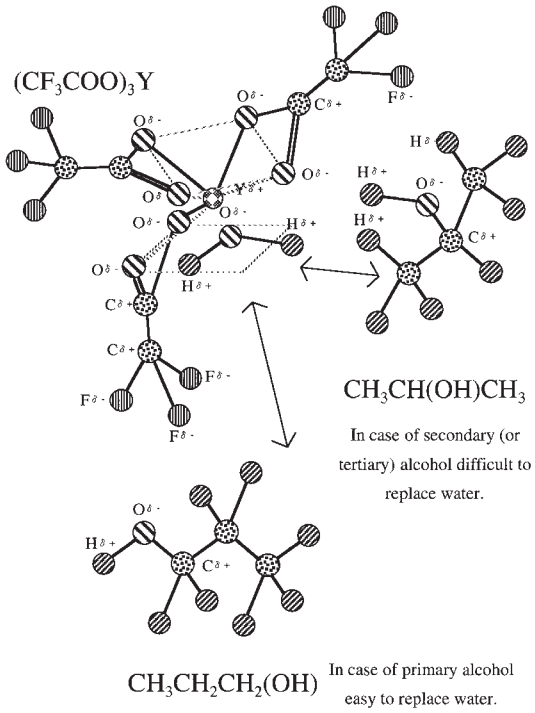

Scheme 1. A presumption of trapping scheme of impurities to Y trifluoroacetates. A yttrium atom is surrounded by three chelating-type bidentateacetate groups and there are open spaces for chemicals to access the yttrium.

3. Impurity Trapping Scheme. The results in Table 3 provided us a surprising fact: that the main impurity was not acetic acid but volatile water. Such a result implied the existence of an unforeseen impurities-trapping scheme. In this scheme, acetic acid vaporized during the purifying process instead of water. Then we considered a scheme of hydrogen bonds between water and yttrium(III) trifluoroacetate, as shown in Scheme 1.[38] Y is surrounded by three chelating-type bidentate acetate groups with open spaces for chemicals to access the central metal of Y.[39] A relatively small molecule of water is considered to be easily trapped nearby the central metal, with Coulomb's force between $O^{\delta-}$ (H_2O) and $Y^{\delta+}$ and two hydrogen bonds of $O^{\delta-}$ (CF_3COO–)–$H^{\delta+}$ (H_2O). In Scheme 1, primary alcohol is also preferable to replace the impurities. However, secondary or tertiary alcohol is not usable because the steric hindrance between carbon chains of alcohol and trifluoroacetates will prevent coordination of $O^{\delta-}$ (–OH) to $Y^{\delta+}$.

It is difficult to confirm the trapping scheme 1 by X-ray diffraction or nuclear magnetic resonance, because of the strong deliquence of the hard and blue gel. As an alternative way, we directly replace the impurities with chemicals and measure the resulting impurities during an additional purifying process. We chose 1-propanol and 2-propanol as replacing materials and obtained two blue gels through common final purifying conditions of 75 °C and 10–20 hPa (vaporization of the higher alcohol made the pressure unstable). By dissolving these blue gels into methanol, we obtain coating solutions D and E, respectively. Amounts of acetic acid, water, 1-propanol, and 2-propanol in D and E are summarized in Table 5.[38] We could not identify the reason why the total amount of acetic acid was larger than the results in Table 3. However, when primary alcohol was used for a replacing material, the water content was lower than that from secondary alcohol. Such results confirm the presumed trapping scheme. Gas chromatography/mass spectroscopy results also revealed the existence of a large amount of higher alcohol; the materials are shown to change into a harmful carbolic group to the YBCO films.[13] Therefore, these replacing materials should not be used for the actual preparation process as far as possible.

4. Purified Coating Solution. These results provide clues for new candidates as replacing materials. The materials should have no steric hindrance to access the central metal and should be able to form hydrogen bonds with the salt. In addition, a material of small molecular weight is desirable because such material is more active for replacing the impurities than a heavy one. According to the above discussion, we concluded that methanol must be the best material as the replacing material. Fortunately, the material is the solvent in the resulting coating solution and therefore never increases the total amount of impurities. Consequently, the SIG method[20] with methanol is concluded to be the ideal method to obtain a purified coating solution. With this method, we can reduce the total amount of the impurities in the coating solution. The purified coating solution has only 0.20 and 0.98 wt % of water and acetic acid, respectively. Figure 2 shows a schematic illustration of TFA-MOD. Gel films prepared by the coating process are calcined and fired to become superconducting YBCO films. Figures 3 and 4 show typical calcining and firing processes, respectively. With the obtained coating solution, we can routinely prepare high-J_c YBCO films having J_c of 5–7 MA/cm^2 (77 K, 0 T) and thickness of 150–230 nm.[18,20]

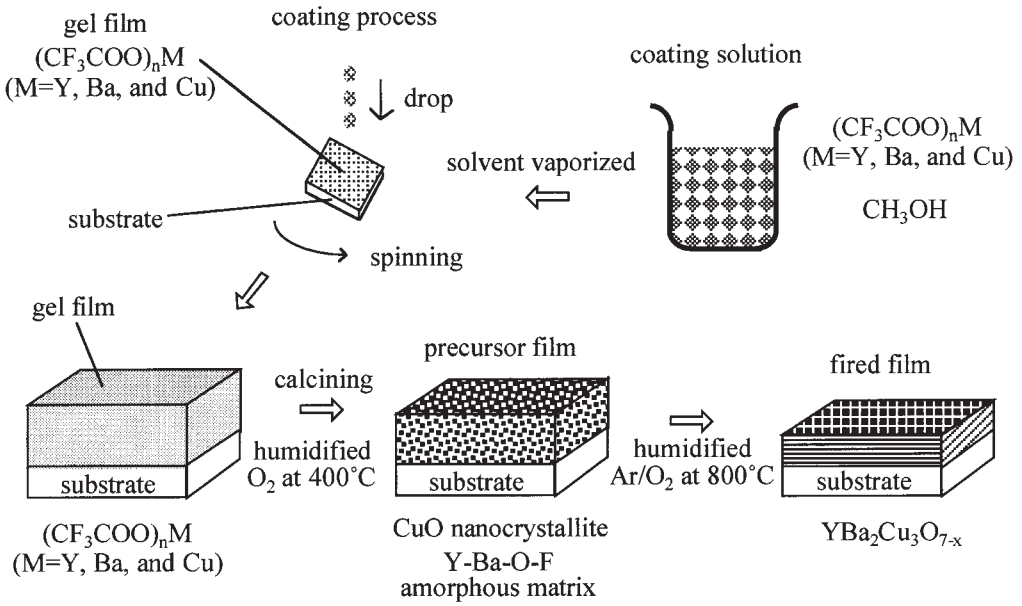

Fig. 2. Schematic illustration of TFA-MOD for fabricating YBCO superconductors. Highly purified coating solution is deposited to give gel film on the substrate by spin-coating. The gel film is calcined to become a precursor film, which consists of CuO nanocrystallites and Y–Ba–O–F amorphous matrix. The precursor film is fired to give YBCO superconductor. All these processes are achieved in ambient pressure.

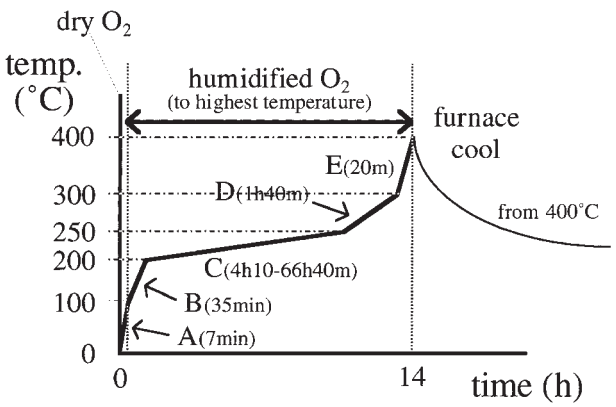

Fig. 3. A typical calcining profile for TFA-MOD. Dry gas is introduced below 100 °C to avoid absorption of water vapor into gel film. Humidified gas above 100 °C partially hydrolyzes Cu trifluoroacetate to avoid its sublimation. All metal trifluoroacetates are decomposed at 200–250 °C to become CuO nanocrystallites and Y–Ba–O–F amorphous matrix. Decomposed harmful residues are expelled above 250 °C.

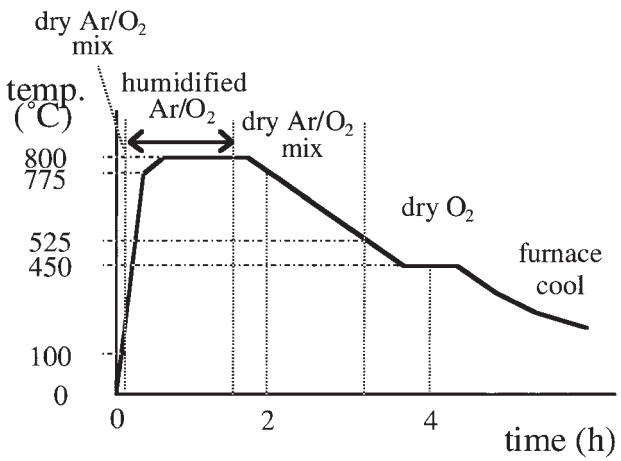

Fig. 4. A firing profile for TFA-MOD. Humidified gas is introduced at 100 °C. Fluorides react with water vapor to generate hydrogen fluoride above 650 °C. YBCO structure forms above 725 °C. An optimal oxygen partial pressure depends on the maximum firing temperature. 1000-ppm oxygen mixed Ar gas is used in the firing profile with a maximum temperature of 800 °C. YBCO film is annealed below 525 °C to become YBCO superconductor.

Growth Scheme of $YBa_2Cu_3O_{7-x}$ during the Firing Process

1. Unsolved Phenomena in TFA-MOD. In TFA-MOD, there are two major phenomena that occur during the firing process, which remain unsolved. Firstly, CuO nanocrystallites in calcined film have no influence on the resulting YBCO structure. Such nanocrystallites induce fatal disorder of the resulting structure in the other MOD processes.[14] Consequently, YBCO film with such disorder has a low-J_c value and its reproducibility is not enough for its application. Secondly, the required firing time is simply proportional to the film thickness. The fact implies that the growth limiting process during the firing process is not diffusion of HF gas in the film between growth front and film surface, but the diffusion from the film surface. Since the content of calcined film in TFA-MOD is similar to the content in the electron beam process, similar chemical reactions during the firing process are expected. In this electron beam process, Solovyov et al. reported the above phenomena.[40,41] Some groups attempted to solve the phenomena by introducing

new models. However, no new model could explain all these phenomena without inconsistency. Prior to our establishing a new model, the reasons why CuO nanocrystallites have no influence on the resulting YBCO structure were studied.

2. CuO Grain Growth. A TEM cross-sectional image of a calcined film that had been calcined for 16h40m at the decomposing temperature of 200–250 °C is shown in Fig. 5.[18] The TEM observation showed CuO nanocrystallites and amorphous matrix. The amorphous matrix consisted of Y, Ba, O, and F atoms and partial Cu content, as detected by energy dispersive X-ray spectrometry. If the diameter depends on the calcining process, it will be natural to think about the grain growth against the time. To detect the CuO nanocrystallites easily, we calcined gel films with four-time duration time at the decomposing temperature. TEM observations of the calcined film are shown in Fig. 6.[18] The average diameter of the CuO nanocrystallite of Fig. 6 seems to be larger than that of Fig. 5. Description of the diameter with an equation is important to predict its growth behavior. Although measuring the real diameter of the CuO nanocrystallite is difficult, a width in a direction has a certain relationship to the diameter. 20 nanocrystallites were measured in both images of Figs. 5 and 6. The obtained average and standard deviation data are summarized in Table 6. The Ostwald ripening scheme predicts the average diameter of grown grain under a condition where only one kind of grain merges with the other to become larger. According to the definition, the time zero must be located in 6h15m at 200–250 °C, when all trifluoroacetates are entirely decomposed to yield oxides.[18] Besides, the scheme requires a fixed temperature during the grain growth. In TFA-MOD, temperature of the calcining process gradually increases so as to decompose the salts effectively. This is only one different condition to apply the Ostwald ripening scheme. Including this one different condition, the diameter follows the equation well. According to the Ostwald ripening scheme,[42] the diameter of a growing grain depends on the heating time described by

$$a_t^3 - a_i^3 = kt. \quad (2)$$

Here, a_t, a_i, t, and k represent the diameter of the growing grain (m), the initial diameter (m), the time (s), and a constant, respectively. From Eq. 2 and the results in Table 6, we calculate k to be 6.12×10^{-29} m^3/s. Even if the initial average diameter of CuO nanocrystallites at 6h15m of the decomposing time in the calcined film were 3 nm at relative large estimation, k is estimated to be 6.11×10^{-29} m^3/s. We can estimate the average size of sample A in Table 6 as 13.2 nm from the datum of sample B. This estimation coincides reasonably well with the result of A shown in the Table 6. The diameter of the CuO nanocrystallite increases with the decomposing time during the calcining process, according to Eq. 2.

3. Indirect Chemical Influence on Superconducting Properties. To study the influence of nanocrystallites on the resulting YBCO structure, we observed some cross-sectional TEM images of the fired film. However, only tightly connected epitaxial layers were observed, when the nanocrystallites grew enough and the diameter of grown nanocrystallite was up to film thickness. Such a result also means that the possibility for capturing the image of the grown grain with cross-sectional

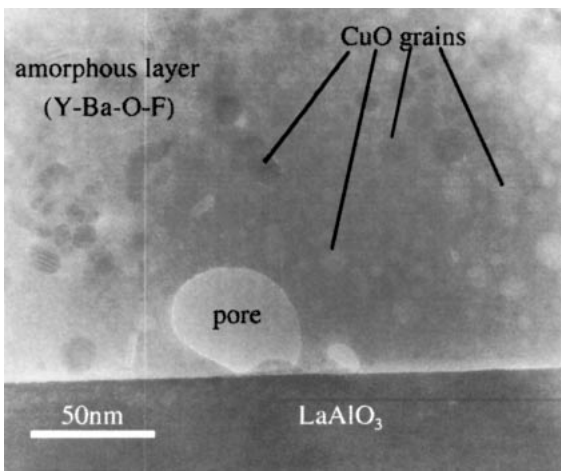

Fig. 5. Cross-sectional TEM observation of precursor film in TFA-MOD. The high spinning rate in spin-coating and solvent vaporization caused the pores on the substrate. In the precursor film, small particles were CuO nanocrystallites and other areas consisted of Y–Ba–O–F amorphous matrix. This figure is reproduced from Fig. 7 of Ref. 18.

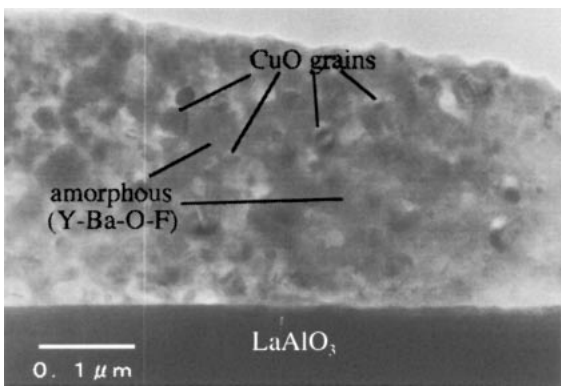

Fig. 6. Cross-sectional TEM observation of YBCO films that were calcined for 66h40m at 200–250 °C during the calcining process. CuO nanocrystallites ripened and grew compared to the film calcined for 16h40m (Fig. 5). This figure is reproduced from Fig. 8 of Ref. 18.

Table 6. Average and Standard Deviation of Nanocrystallite Size in Precursors

Sample	Duration time[a)] at 200 to 250 °C /h	Average grain size /nm	Standard deviation of grain size /nm
A	10.4	14.0	1.33
B	60.4	23.7	6.56

a) Calculated by subtracting the decomposed time (6.3 h) from the calcining time.

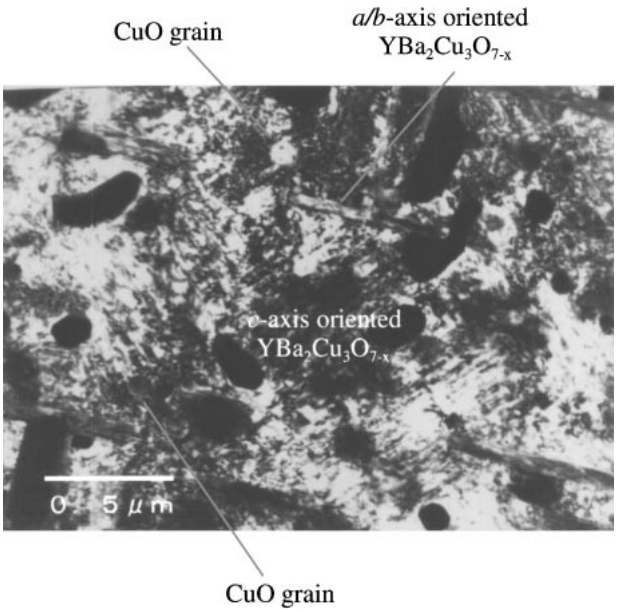

Fig. 7. Plan-view TEM observation of the fired film, which was calcined for 66h40m. *c*-Axis-oriented $YBa_2Cu_3O_{7-x}$ grains grew perfectly around CuO grains. The observed microstructure supports the high reproducibility in high-J_c of the films prepared by TFA-MOD. This figure is reproduced from Fig. 2 of Ref. 19.

images is small. Based on this idea, a plan-view TEM image of the film derived from a long-calcined one was observed. The plan-view observation is shown in Fig. 7.[19] The film shows tightly connected *c*-axis-oriented YBCO grains as a matrix, *a*/*b*-axis-oriented YBCO grains, and large CuO grains from chemical microanalysis by energy dispersive X-ray spectrometry. The content of areas except CuO grains was stoichiometric. Dark areas, where no material exists, derived from the sample preparation process or from the rough surface of the fired film. Therefore, the total content of the observed area is non-stoichiometric. At that time, the reason was not clear. However, the reason why we could not find the CuO grains when we used some cross-sectional images was clear: the film has only a few gigantic CuO grains within one observed area. These gigantic grains physically disturb the superconducting current. In addition, YBCO film on $LaAlO_3$ intrinsically has a large amount of *a*/*b*-axis-oriented YBCO grains, which never carry superconducting current. Such obstacles enhance the influence of the CuO grain as a physical obstacle in the fired film. To study the influence, J_c dependence on the decomposing time during the calcining process was studied; the result is summarized in Fig. 8. However, the influence was much stronger than the above assumption. Figure 7 shows that J_c of the film with the CuO grain decreases by 30% at maximum estimation even if *a*/*b*-axis-oriented grains enhanced the influence of the grown CuO obstacles. Results in Fig. 8 imply an unforeseen phenomenon. The result of Fig. 7 also implies undiscovered Y and Ba compounds because of the stoichiometric content. From the other cross-sectional images of the fired film, perfectly epitaxial growth on the substrate is always observed. From such a viewpoint, we conclude that Y and Ba compounds exist on the YBCO layer and near the surface, because stoichiometric layer and

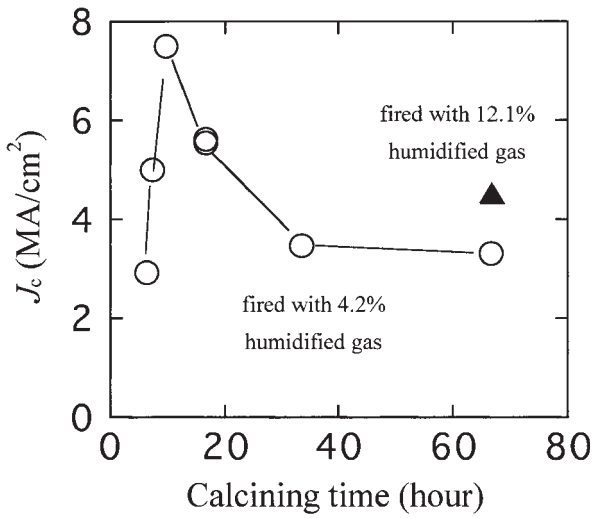

Fig. 8. Dependence of J_c of the resulting films on the calcining time at 200–250 °C. J_c increased with calcining time below 9h43m and then decreased with longer calcining times above 9h43m. This result does not agree with the decomposition of metal trifluoroacetates. Some undetected residues might cause the deterioration of J_c. The J_c of the long-calcined film, fired with 12.2% humidified gas, was slightly improved but not perfectly restored. An appropriate calcining time is indispensable in obtaining high-J_c YBCO films. This figure is reproduced from Fig. 1 of Ref. 19.

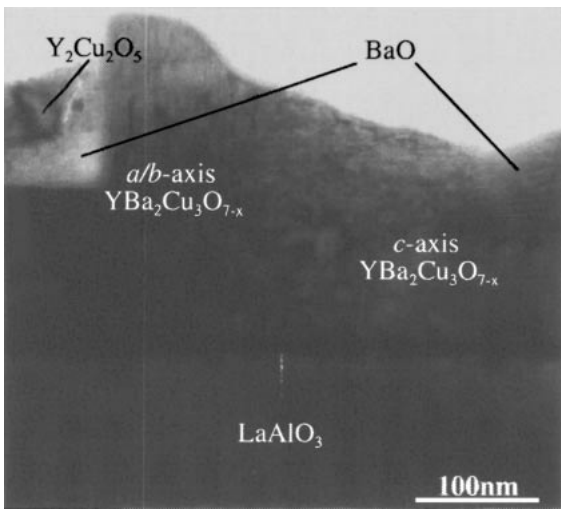

Fig. 9. Cross-sectional TEM observation of YBCO film by TFA-MOD. The film was prepared with the highly purified coating solution by the SIG method. On the substrate, perfectly *c*-axis-oriented YBCO grains were observed. *a*/*b*-Axis-oriented grains were also observed on the *c*-axis-oriented grains. The other phases were observed near the surface and these phases derived from non-stoichiometric quasi-liquid during firing. This figure is reproduced from Fig. 13 of Ref. 18.

CuO grains exist on the substrate. To confirm the existence of Y and Ba compounds, we observed a cross-sectional TEM image including both substrate and rough surface of a fired film. The image shown in Fig. 9 showed epitaxial growth of *c*-axis-ori-

ented YBCO grains on the surface, and the figure also shows *a*/*b*-axis-oriented YBCO grains and the other phases, which are Y and Ba compounds, on the layer. In this figure, although CuO grains were not observed, stoichiometric content also implies their existence in the other area. Such indirect chemical influence of CuO grains mainly degrades J_c values of the fired film.

4. Growth Scheme of Epitaxial YBCO in TFA-MOD. TFA-MOD has some characteristic growth modes of YBCO layer. YBCO layer formed near the substrate without any problem, but did not form near the surface. YBCO layer began to form on the substrate toward the top of the film. These results provided me with important clues to discover the characteristic growth scheme. Some groups considered that an intermediate state appears only near the growth front of the YBCO grains. Their assumption was quite natural. On the growth front, new grains can easily form because of Coulomb's force. However, according to this growth mode, the possibility for formation of the other phase must be uniform within the film. Yet actual results revealed no other phases near the substrate. Based on such results, we conclude that the intermediate layer must form in all the film during the firing process, so Coulomb's force near the growth front is not dominant enough to form a new layer. The intermediate state is called a quasi-liquid. During the firing process, YBCO growth requires water vapor and HF gas is simultaneously released. Moreover, fluorine ion sensor studies suggest that fluoride is generated above a certain temperature. Therefore, I could presume that the formation of the quasi-liquid requires six kinds of atoms, which are Y, Ba, Cu, O, F, and H, at higher temperatures. Each atom has a range in the concentration to form the quasi-liquid. Since a group reported that the chemical reactions during the firing process are in equilibrium,[28] formation of the quasi-liquid must be in equilibrium from the raw material to the YBCO grain. The expected chemical reactions are described below:

$$\mathrm{CuO} + \text{matrix (Y, Ba, O, and F)} + \mathrm{H_2O} \leftrightarrow \text{quasi-liquid (Y, Ba, Cu, O, H, and F)} \quad (3a)$$

$$\text{quasi-liquid (Y, Ba, Cu, O, H, and F)} \leftrightarrow \mathrm{YBCO} + \mathrm{HF}\uparrow. \quad (3b)$$

A quasi-liquid network forms in the film during the firing process, based on the above presumption, as shown in Scheme 2(a).[19] This quasi-liquid network helps transportation of water and HF in the film, as shown in Eqs. 3a and 3b. The quasi-liquid only releases YBCO grains on lattice-matched areas because of Coulomb's force. This growth scheme permits both *c*-axis-oriented and *a*/*b*-axis-oriented grains on the substrate. The growth

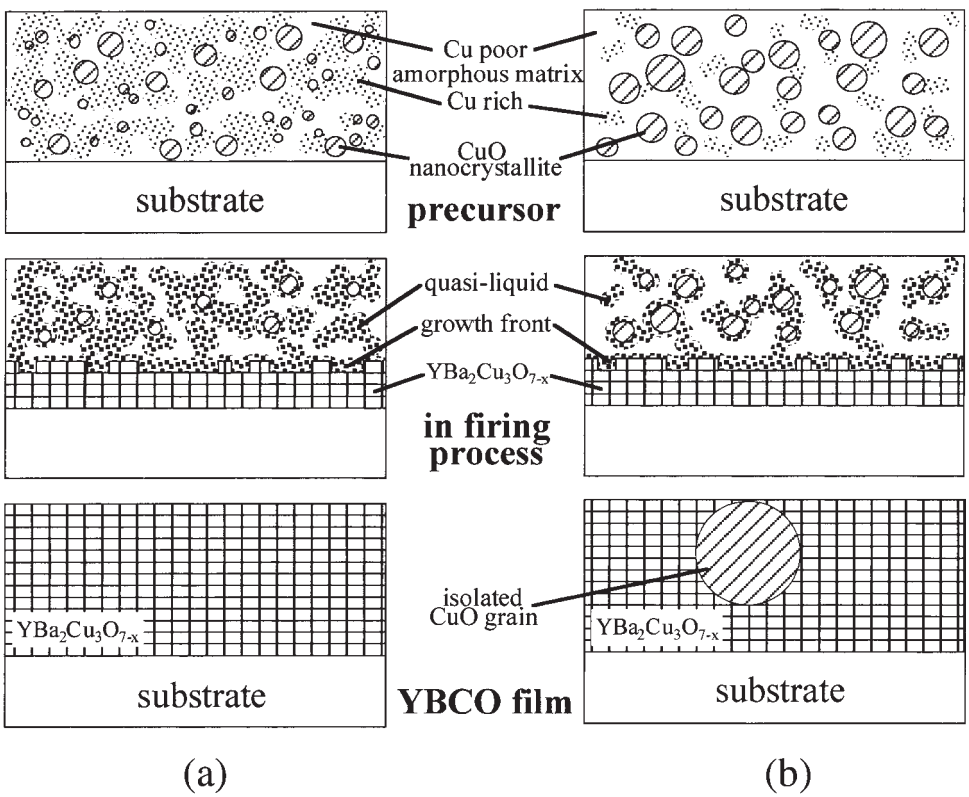

Scheme 2. Growth mechanism of $YBa_2Cu_3O_{7-x}$ grains prepared by TFA-MOD during firing. Precursor films calcined for (a) a suitable time and (b) a long time. Precursor (b) has many large CuO nanocrystallites but few amorphous regions, which are Cu-rich compared to precursor (a). During the firing process, quasi-liquid forms in the Cu-rich amorphous region and CuO/amorphous interface. The diameter of the CuO nanocrystallites decreases to form the quasi-liquid. The quasi-liquid releases YBCO grains and HF gas only on the YBCO growth front because of energetic stability. The quasi-liquid also supports the transportation of HF and H_2O between the precursor's surface and YBCO growth front. The resulting YBCO film has almost perfectly *c*-axis-oriented YBCO grains and permits the existence of isolated CuO grains. This structure leads to high J_c of the YBCO film with high reproducibility. This scheme is reproduced from Fig. 3 of Ref. 19.

rate in the vertical direction of the a/b-axis-oriented grains is much faster than that in the horizontal direction. Since the growth of a/b-axis-oriented grains reached a maximum before a large volume reduction of the film during the firing process, the surface of the film becomes always rough, as shown in Fig. 9. An optimally calcined film shown in Scheme 2(a) yields a small number of gigantic CuO grains in the fired film. On the other hand, the film in Scheme 2(b) calcined for a long time yields a relative large number of CuO grains; thus, the resulting YBCO film has a low-J_c result. Decomposition of trifluoroacetates and vaporization of the resulting harmful resides requires at least about 10 hours, as we reported.[18] During this time, CuO nanocrystallites inevitably merge with each other to make larger ones. Such larger CuO nanocrystallites have an influence on YBCO thickness. Scheme 3 shows that the non-stoichimetric area has indirect influence on YBCO layer because the other phases can form on it. Schemes 3(a) and (b) show the growth mode of a properly calcined film. At the beginning of the firing process, a small nanocrystallite has no influence, because a small difference to the stoichiometry is permitted to form the quasi-liquid. Nevertheless, around the end of the film growth, increased concentration of Cu content by the small CuO nanocrystallite breaks the condition for the quasi-liquid. Consequently, a properly calcined film has small other phases on it. In the case of a film calcined for a long time, a large amount of the other phases forms, as illustrated in Schemes 3(c) and 3(d). The thickness of the YBCO layer decreases and the J_c of the YBCO film degrades. The explanation with the quasi-liquid network model is entirely consistent with the actual results. High-J_c film shows strong YBCO peaks when studied by XRD.

5. Conditions Required to Obtain High-J_c YBCO Film. This study revealed that J_c of the YBCO film depends on the decomposing time during the calcining process. On this issue, two groups have reported no influence of the calcining process.[43,44] Only in our group, impurities are reduced, as shown in the former section. To investigate the reason, I dared to prepare a non-purified coating solution without SIG method and fired a YBCO film with the coating solution. Figure 10 shows a cross-sectional image of the film obtained. The YBCO film has Y and Ba compounds in the film. The intermediate locations of these compounds meant that these compounds derived, not from non-stoichiometric contents in the quasi-liquid as shown in Scheme 3, but from impurities in the coating solution. This film must have a large amount of the other phase on the film due to indirect chemical influence. Even if CuO nanocrystallites were reduced by the optimal calcining process, the other particles of Y and Ba compounds remain in the film, as shown in Fig. 10. The effect of only the CuO reduction by the optimal process is subtle. Two groups could not find any effect because of the Y and Ba compounds.[43,44] A combination of coating solution highly purified by SIG method and the optimal calcining process is required to obtain high-J_c YBCO film.[33]

6. Suppression of Influence of CuO Nanocrystallites. The quasi-liquid network model explained all unsolved problems in TFA-MOD discussed above. To improve the J_c value of the film and to confirm the model, we performed an additional experiment. A calcined film that was calcined for a long time at the decomposing temperature has relative large CuO nanocrys-

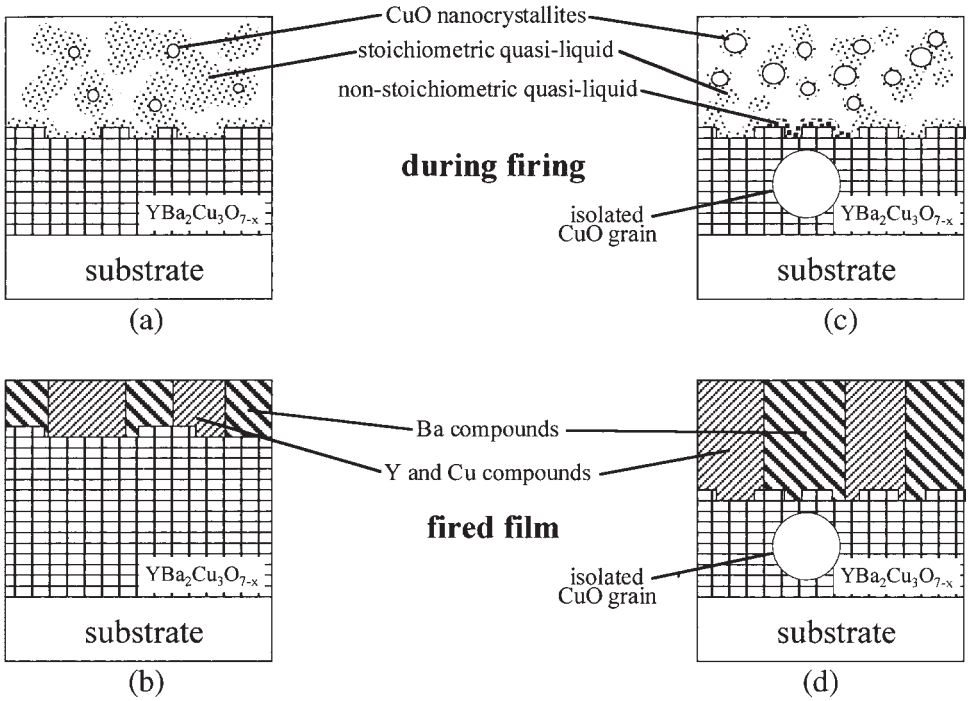

Scheme 3. Schematic illustration of YBCO growth from precursor film with small CuO nanocrystallites (a), (b) and large ones (c), (d). In the precursor film with small nanocrystallites (a), YBCO grows to the substrate surface without problems. However, non-stoichiometric quasi-liquid, derived from CuO nanocrystallites, near the surface leads to non-superconducting phases (b). In the precursor with large nanocrystallites (c), Y- and Ba-rich quasi-liquid forms during the firing process. Consequently in (d), thicker non-YBCO layer forms on the YBCO layer compared with the case for small nanocrystallites. CuO grains in the fired film indirectly degrade its J_c. This scheme is reproduced from Fig. 12 of Ref. 18.

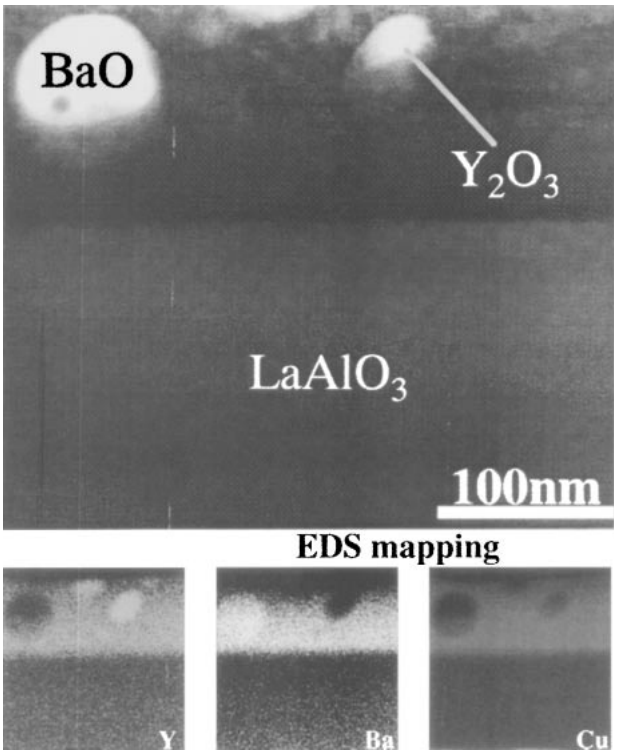

Fig. 10. Cross-sectional TEM image with EDS mappings of the YBCO film derived from normally purified coating solution without applying the SIG method. Observed Ba and Y oxides deteriorated the J_c of the film. Even if the optimal calcining profile suppresses the CuO grains in fired film, J_c of the film hardly improves. This figure is reproduced from Fig. 4 of Ref. 33.

tallites and the nanocrystallites merge with each other into larger CuO grains during the firing process. With an effective way to decrease the CuO nanocrystallites during the firing process, J_c of the resulting YBCO film must be improved. Since the chemical reaction is in equilibrium, Eq. 3a has an equilibrium constant. Although the constant depends on the firing temperature, the dependence is unclear. On the other hand, CuO nanocrystallites are converted to become a quasi-liquid by increasing reacting materials at a certain temperature. Among the starting materials, only water content can easily be increased. A long-calcined film was fired under very humidified atmosphere based on this idea. The result is also shown in Fig. 8 using filled triangles. J_c improvement confirmed the quasi-liquid network model, but the improvement was imperfect compared with the maximum value. Consequently, the optimal calcining process is indispensable to obtain high-J_c results.

Conclusions

When one plans to prepare purified coating solution for TFA-MOD, a base-exchanging route is one of the best ways because trifluoroacetates esterify with alcohol solvent. During the purifying process, 10–12 wt % impurities of water and acetic acid remain in the glassy blue gel. The main impurity is not acetic acid but volatile water. Water is presumed to be collected around the central metal of trifluoroacetate with hydrogen bonds. The conditions required for replacing material include the absence of any steric hindrance which would prevent access the central metal of trifluoroacetate and hydrogen bonds. Methanol fulfills such conditions; furthermore the material is the final solvent, so it will never increase the total amount of impurities. With this replacing material, water content was reduced from 3.4 to 0.20 wt %. With the purified coating solution, YBCO films having J_c of 5–7 MA/cm^2 (77 K, 0 T) are routinely obtained.

During the firing process of TFA-MOD, a quasi-liquid network plays important roles. The network helps transportation of water and HF gas, suppresses the influence of small CuO nanocrystallites on J_c of the resulting YBCO film, and helps epitaxial growth of YBCO layer. Large nanocrystallites in calcined film merge with each other to become gigantic CuO grains in the fired film. The diameter of the CuO grains was up to 150 nm, as large as the YBCO film thickness. The CuO nanocrystallites in the calcined film deteriorate the J_c value of the resulting YBCO film in two modes: one is creating physical obstacles and the other is indirect chemical influence. In the latter mode, non-stoichiometric quasi-liquid derived from the CuO changes into the other phases of YBCO near the surface. YBCO film derived from coating solution without purifying process has Y and Ba compounds far from the surface in the YBCO structure. The optimal calcining process improves the J_c of the above film very little, because indirect chemical influence from Y and Ba compounds is predominant. The conditions required to obtain high-J_c YBCO film are a combination of highly purified coating solution and the optimal calcining process. Excess humidity during the firing process is effective to reduce the influence of CuO nanocrystallites. However, the effect is inadequate. To obtain high-J_c YBCO film, an optimal calcining process is indispensable.

The author is grateful for discussions on CuO ripening schemes and YBCO growth models with Dr. Izumi Hirabayashi. This work was partially supported by the New Energy and Industrial Technology Development Organization (NEDO) as Collaborative Research and Development of Fundamental Technologies for Superconductivity Applications.

References

1 C. Buzea and T. Yamashita, *Supercond. Sci. Technol.*, **14**, R115 (2001).

2 S. J. Golden, F. F. Lange, D. R. Clarke, L. D. Chang, and C. T. Necker, *Appl. Phys. Lett.*, **61**, 351 (1992).

3 S. Chromik, A. Sin, V. Strbik, G. Plesch, P. Odier, and F. Weiss, *Supercond. Sci. Technol.*, **14**, 875 (2001).

4 A. Usoskin, J. Dzick, A. Issaev, J. Knoke, F. Garcia-Moreno, K. Sturm, and H. C. Freyhardt, *Supercond. Sci. Technol.*, **14**, 676 (2001).

5 J. Knauf, R. Semerad, W. Prusseit, B. DeBoer, and J. Eickemeyer, *IEEE Trans. Appl. Supercond.*, **11**, 2885 (2001).

6 Y. Iijima, K. Kakimoto, M. Kimura, K. Takeda, and T. Saitoh, *IEEE Trans. Appl. Supercond.*, **11**, 2816 (2001).

7 Y. Yamada, S. B. Kim, T. Araki, Y. Takahashi, T. Yuasa, H. Kurosaki, I. Hirabayashi, Y. Iijima, and K. Takeda, *Physica C*, **357–360**, 1007 (2001).

8 Y. Yamada, T. Araki, H. Kurosaki, S. B. Kim, T. Yuasa, Y. Shiohara, I. Hirabayashi, Y. Iijima, T. Saitoh, J. Shibata, Y.

Ikuhara, T. Katoh, and T. Hirayama, *Adv. Cryog. Eng.*, **48**, 631 (2002).
9 T. Kumagai, T. Manabe, W. Kondo, H. Minamiue, and S. Mizuta, *Jpn. J. Appl. Phys.*, **29**, L940 (1990).
10 T. Manabe, I. Yamaguchi, S. Nakamura, W. Kondo, T. Kumagai, and S. Mizuta, *J. Mater. Res.*, **10**, 1635 (1995).
11 M. F. Ng, S. C. Peterson, and M. J. Cima, *Mat. Res. Soc. Symp. Proc.*, **169**, 731 (1990).
12 P. Boullay, B. Domenges, M. Hervieu, and B. Raveau, *Chem. Mater.*, **5**, 1683 (1993).
13 F. Parmigiani, G. Chiarello, N. Pipamonti, H. Goretzki, and U. Roll, *Phys. Rev. B*, **36**, 7148 (1987).
14 J. Shibata, K. Yamagiwa, I. Hirabayashi, X. Ma, J. Yuan, T. Hirayama, and Y. Ikuhara, *Jpn. J. Appl. Phys.*, **38**, 5050 (1999).
15 Y. Masuda, R. Ogawa, Y. Kawate, K. Matsubara, T. Tateishi, and S. Sakka, *J. Mater. Res.*, **8**, 693 (1993).
16 A. Gupta, R. Jagannathan, E. I. Cooper, E. A. Giess, J. I. Landman, and B. W. Hussey, *Appl. Phys. Lett.*, **52**, 2077 (1988).
17 P. C. McInytre, M. J. Cima, J. A. Smith, Jr., R. B. Hallock, M. P. Siegal, and J. M. Phillips, *J. Appl. Phys.*, **71**, 1868 (1992).
18 T. Araki, T. Niwa, Y. Yamada, I. Hirabayashi, J. Shibata, Y. Ikuhara, K. Kato, T. Kato, and T. Hirayama, *J. Appl. Phys.*, **92**, 3318 (2002).
19 T. Araki, I. Hirabayashi, J. Shibata, and Y. Ikuhara, *Supercond. Sci. Technol.*, **15**, 913 (2002).
20 T. Araki, K. Yamagiwa, K. Suzuki, I. Hirabayashi, and S. Tanaka, *Supercond. Sci. Technol.*, **14**, L21 (2001).
21 D. T. Verebelyi, U. Schoop, C. Thieme, X. Li, W. Zhang, T. Kodenkandath, A. P. Malozemoff, N. Nguyen, E. Siegal, D. Buczek, J. Lynch, J. Scudiere, M. Rupich, A. Goyal, E. D. Specht, P. Martin, and M. Paranthaman, *Supercond. Sci. Technol.*, **16**, L19 (2003).
22 J. T. Dawley, P. G. Clem, M. P. Siegal, D. R. Tallant, and D. L. Overmyer, *J. Mater. Res.*, **17**, 1900 (2002).
23 M. Falter, W. Haessler, B. Schlobach, and B. Holzapfel, *Physica C*, **372–376**, 46 (2002).
24 O. Castano, A. Cavallaro, A. Palau, J. C. Gonzalez, M. Rossell, T. Puig, F. Sandiumenge, N. Mestres, S. Pinol, A. Pomar, and X. Obradors, *Supercond. Sci. Technol.*, **16**, 45 (2003).
25 T. Izumi, T. Honjo, Y. Tokunaga, H. Fuji, R. Teranishi, Y. Iijima, T. Saitoh, Y. Nakamura, and Y. Shiohara, *IEEE Trans. Appl. Supercond.*, **13**, 2500 (2003).
26 P. M. Mankiewich, J. H. Scofield, W. J. Skocpol, R. E. Howard, A. H. Dayem, and E. Good, *Appl. Phys. Lett.*, **51**, 1753 (1987).
27 R. Feenstra, T. B. Lindemer, J. D. Budai, and M. D. Galloway, *J. Appl. Phys.*, **69**, 6569 (1991).
28 V. F. Solovyov, H. J. Wiesmann, L. Wu, Y. Zhu, and M. Suenaga, *Appl. Phys. Lett.*, **76**, 1911 (2000).
29 P. C. McIntyre, M. J. Cima, and M. F. Ng, *J. Appl. Phys.*, **68**, 4183 (1990).
30 P. C. McIntyre, M. J. Cima, D. H. Liebenberg, and T. L. Francavilla, *Appl. Phys. Lett.*, **58**, 2033 (1991).
31 J. A. Smith, M. J. Cima, and N. Sonnenberg, *IEEE Trans. Appl. Supercond.*, **9**, 1531 (1999).
32 M. P. Siegal, P. G. Clem, J. T. Dawley, R. J. Ong, M. A. Rodriguez, and D. L. Overmyer, *Appl. Phys. Lett.*, **80**, 2710 (2002).
33 T. Araki, T. Kato, T. Muroga, T. Niwa, T. Yuasa, H. Kurosaki, Y. Iijima, Y. Yamada, T. Hirayama, T. Saitoh, Y. Shiohara, and I. Hirabayashi, *IEEE Trans. Appl. Supercond.*, **13**, 2803 (2003).
34 P. Calvert and M. J. Cima, *J. Am. Ceram. Soc.*, **73**, 575 (1990).
35 J. T. Dawley, R. J. Ong, and P. G. Clem, *J. Mater. Res.*, **17**, 1678 (2002).
36 T. Araki, K. Yamagiwa, and I. Hirabayashi, *Cryogenics*, **41**, 675 (2001).
37 The Chemical Society of Japan, "Kagaku-Binran Kiso-hen, 3rd ed (in Japanese)," Maruzen Kabushiki-kaisya, Tokyo (1984).
38 T. Araki and I. Hirabayashi, *Chem. Mater.*, submitted (2003).
39 A. Lossin and G. Z. Meyer, *Anorg. Allg. Chem.*, **69**, 1603 (1993).
40 V. F. Solovyov, H. J. Wiesmann, and M. Suenaga, *Physica C*, **353**, 14 (2001).
41 V. F. Solovyov, H. J. Wiesmann, L. Wu, Y. Zhu, and M. Suenaga, *IEEE Trans. Appl. Supercond.*, **11**, 2939 (2001).
42 G. P. Wirtz and M. E. Fine, *J. Am. Ceram. Soc.*, **51**, 402 (1968).
43 P. C. McIntyre and M. J. Cima, *J. Mater. Res.*, **9**, 2219 (1994).
44 J. T. Dayley, P. G. Clem, M. P. Siegal, D. L. Overmyer, and M. A. Rodriguez, *IEEE Trans. Appl. Supercond.*, **11**, 2831 (2001).

Takeshi Araki is born in Sendai, Miyagi, Japan, in 1966. He received a B.Eng. from the University of Tokyo in 1990. At 1990, he joined Research & Development Center of TOSHIBA Corp. He researched and developed fuel cell technology till 1998. He temporarily transferred to division V of Superconductivity Research Laboratory in Nagoya from 1998 to 2003. He is now temporarily transferred to Material Science and Physics division of the same institution in Tokyo this April. He has studied a chemical solution process to fabricate $YBa_2Cu_3O_{7-x}$ superconductor since 1999. His current research interests are chemical reactions to expel harmful carbon contents and growth scheme of epitaxial layer in the solution process. He received The Presentation Award from Cryogenic Association of Japan in 2001, The Outstanding Young Investigator from the same society in 2002, and The CSJ Award for Young Chemists in Technical Development in 2002.